EXPERIMENTAL STUDIES OF INTERNAL AND NEAR-BED DYNAMICS OF RESTRICTED EXCHANGE FLOWS

Magda Carr, Alan Cuthbertson, Janek Laanearu, Joël Sommeria, Jonathan Kean, Madis-Jaak Lilover, Monika Kollo, Jarle Berntsen, Øyvind Thiem, Samuel Viboud

E-proceedings of the 36th IAHR World Congress
28 June – 3 July, 2015, The Hague, the Netherlands

EXPERIMENTAL STUDIES OF INTERNAL AND NEAR-BED DYNAMICS OF RESTRICTED EXCHANGE FLOWS

MAGDA CARR[(1)], ALAN CUTHBERTSON[2)], JANEK LAANEARU[(3)], JOEL SOMMERIA[(4)], JONATHAN KEAN[(2)], MADIS-JAAK LILOVER[(5)], MONIKA KOLLO[(3)], JARLE BERNTSEN[(6)], ØYVIND THIEM[(7)] & SAMUEL VIBOUD[(4)]

[(1)] *School of Mathematics, University of St Andrews, St Andrews, UK,*
e-mail magda@mcs.st-and.ac.uk

[(2)] *School of Energy, Geosciences, Infrastructure and Society, Heriot Watt University, Edinburgh, UK,*
e-mail a.cuthbertson@hw.ac.uk

[(3)] *Department of Mechanics, Tallinn University of Technology, Tallinn, Estonia,*
e-mail janek.laanearu@ttu.ee

[(4)] *Laboratoire des Ecoulements Géophysiques et Industriels, Grenoble, France,*
email joel.sommeria@legi.grenoble-inp.fr

[(5)] *Institute of Marine Systems, Tallinn, Estonia,*
email madis@phys.sea.ee

[(6)] *Department of Mathematics, University of Bergen, Bergen, Norway,*
email jarleb@math.uib.no

[(7)] *Uni Research AS, Bergen, Norway,*
email: oyvind.thiem@uni.no

ABSTRACT

Results are presented from a series of experiments investigating the internal and near-bed dynamics of restricted net exchange flows across a submerged sill obstruction. Experimental measurements focused on obtaining high-resolution velocity and density profiles in the vicinity of the obstruction to observe and quantify both interfacial mixing and boundary layer processes under a range of parametric forcing conditions (i.e. variable saline and fresh water flow rates; density differences; water levels). Detailed synoptic velocity fields were also measured across the obstruction through particle image velocimetry (PIV) to aid qualitative and quantitative interpretation of these internal and near-bed flow processes, with a focus on defining the specific parametric conditions under which saline intrusions could become arrested through erosion of the intrusion nose at the bed boundary by the freshwater outflow layer. In this regard, it is anticipated that the study findings will provide an important step towards achieving improved representation of interfacial mixing and boundary layer processes within semi-enclosed estuaries and fjords, which are often poorly represented in current numerical models.

Keywords: Exchange flows; stratification; interfacial mixing; boundary layer; estuaries.

1. INTRODUCTION

The presence of natural topographic flow obstructions has a strong influence on the intrusion of saline marine waters into semi-enclosed brackish estuarine impoundments or stratified fjordic basins. This restricted exchange can suppress estuarine or fjordic circulation and mixing processes, leading to stagnation and contaminant (e.g. nutrient) accumulation problems within impoundments (e.g. Cuthbertson et al., 2004; 2006), thus impacting adversely on estuarine/fjordic ecology. Field studies conducted in the Baltic Sea region (e.g. Lilover et al., 1998; Laanearu et al., 2007; 2011) have indicated different stratified flow patterns in semi-enclosed estuaries, with extensive mixing observed near permanent salinity fronts (Lilover & Stips 2008). Consequently, some obstructed estuaries can be completely blocked from marine saline water intrusion into the semi-enclosed impoundment, while others are strongly influenced by saline water circulations at the river mouth, with restricted intrusion into the estuary basin flowing in the opposite direction to the overlying freshwater outflow layer (e.g. Sargent and Jirka, 1988), as shown schematically in Figure 1.

In this regard, the internal flow and near-bed dynamics associated with these restricted exchange flows are expected to be influenced by (i) the overall dimensions, submergence and rigidity/erodibility/roughness of the obstruction, (ii) the initial density and stratification differences between the two water bodies, and (iii) the external forcing conditions due to tidal saline intrusion and river freshwater inflows. However, limited information exists, as yet, as to range of parametric conditions under which these restricted exchange flows are initiated (or indeed blocked). Research is also required to investigate the physical mechanisms associated with shear-induced mixing processes and vertical entrainment by bi-directional flows across submerged obstructions.

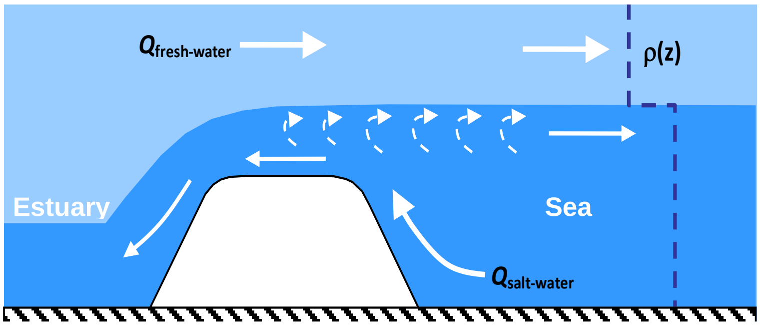

Figure 1. Schematic representation of a counterflowing, restricted exchange flow across a submerged obstruction within a partially blocked estuary.

2. EXPERIMENTAL FACILITY AND SET-UP

The experimental program, funded under the EU FP7 Hydralab IV Initiative, was conducted in the largest rotating platform in the world; the LEGI Coriolis Platform II in Grenoble. Access to this facility provided a unique opportunity to conduct large-scale (i.e. high Reynolds number) physical modelling of environmental and geophysical flow problems, such as restricted exchange flow dynamics, in the presence of density stratification and bottom topography.

The circular tank mounted on the Coriolis rotating platform is 13 m in diameter and 1.2 m-deep (allowing water depths up to a maximum of 1 m). Rotating angular speed for the basin can be varied between 0 and 6 rpm (corresponding to angular velocities $\Omega = 0 – 0.5\ s^{-1}$). For the current experimental study, conducted mostly under non-rotating conditions, a 9 m-long by 1.5 m-wide by 1.2 m-deep rectangular channel was constructed within the basin (see Figure 2). This channel incorporated a rigid trapezoidal obstruction with a 2 m-long horizontal sill of height h_s = 0.5 m and approach slopes of 27.2° [Figure 2(a)]. The walls of the central 6 m-long section of the channel, along with the obstruction, were constructed from transparent Plexiglas to facilitate laser flow illumination and visualization.

Within the estuarine run configuration considered herein, counter-flowing layers of saline water (ρ_1 = 1004.7 – 1009.6 kg/m^3) and overlying freshwater (ρ_0 = 1000 – 1001.1 kg/m^3) were generated across the obstacle sill. The saline water was delivered to the channel via a gravity feed system and was injected directly into the bottom of the sea basin through rectangular manifold section [Figure 2(a)], while fresh ambient water was recirculated within the channel and the surrounding circular tank by two centrifugal pumps located in the upper sea basin [Figure 2(b)]. These two injection systems provided brine and freshwater inflow rates of Q_1 = 10 - 25 l/s and Q_0 = 0 – 30 l/s, respectively.

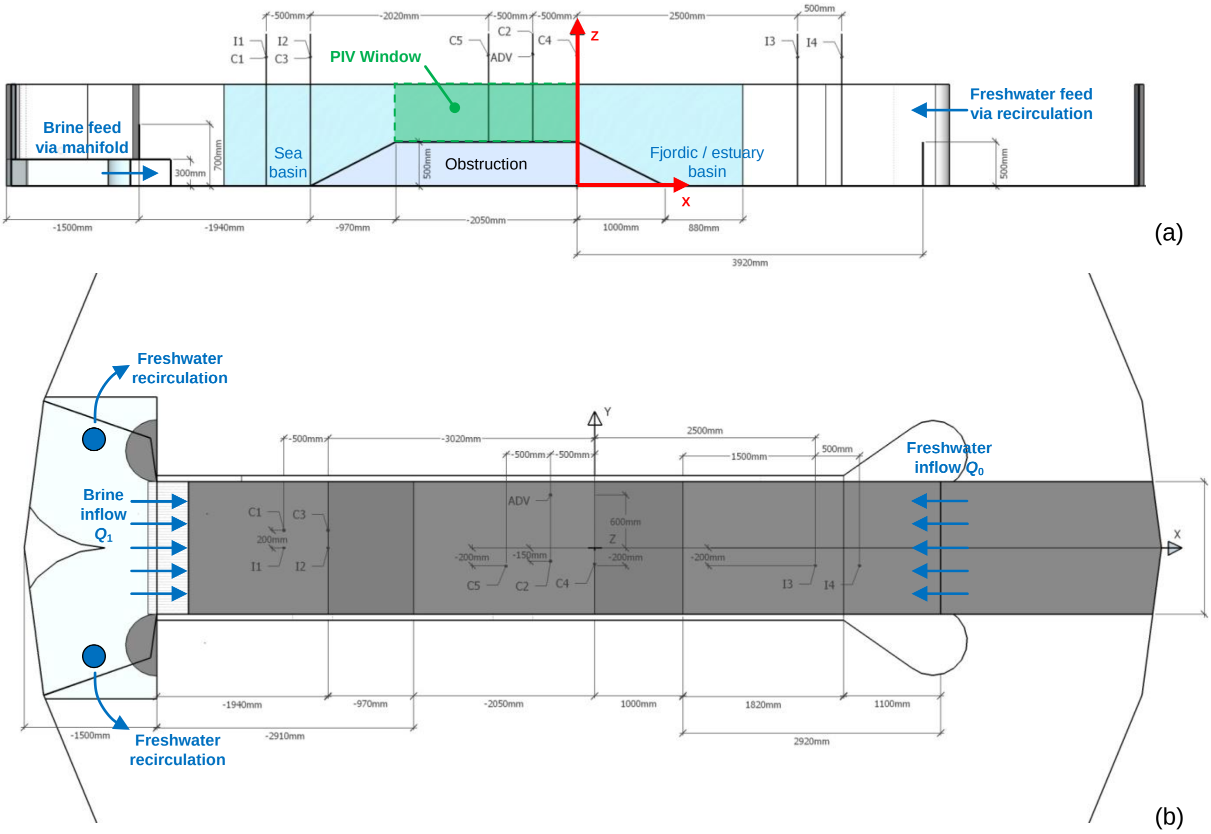

Figure 2. Schematic representation of the experimental set-up and instrumentation locations: (a) side view and (b) top view, showing directions of counter-flowing freshwater and brine inputs. Note: the figure orientation is opposite to that shown in Figure 1.

The initial experimental configuration for the estuary runs was one in which circular tank and channel were initially filled with quiescent ambient freshwater. The saline water was then carefully fed into bottom of the sea basin, avoiding excessive initial mixing with the ambient freshwater volume. Once the saline water layer thickness had reached the sill crest elevation (i.e. 0.5 m), the gravity-driven feed rate of saline water was increased to the desired inflow rate Q_1. At this point a dense water overflow developed across the sill obstruction spilling into the estuary/fjordic basin, which, after a short period of time (1 - 2 minutes typically), reached a quasi-steady condition (for the Q_0 = 0 case). Subsequently, the freshwater inflow was increased incrementally (i.e. $Q_0 = 0 \rightarrow 3 \rightarrow 11 \rightarrow 18 \rightarrow 26 \rightarrow 30$ l/s) at prescribed times during the experimental run, with corresponding quasi-steady exchange flow conditions achieved in each case. Thus, the parametric dependence of the exchange flow conditions developed across the sill was tested in relation to (i) the relative submergence depth of the sill h_s/H (= 0.5 - 0.6); (ii) the relative density difference of the fresh and salt water inflows $(\rho_1 - \rho_0)/\rho_0$ (= 0.005 - 0.01); and (iii) the relative magnitude of fresh and saline inflows Q_0/Q_1 (= 0 - 1.2).

Experimental measurements focused mainly on obtaining high temporal and spatial resolution density and velocity fields both across the sill obstruction and within the estuarine/fjordic and sea water basins on either side of the obstruction for the different exchange flow conditions tested. Flow illumination was provided by a laser system sited at the far end of the estuarine/fjordic basin, which produced a vertical laser light sheet aligned along the channel centerline (see Figure 2). Two-dimensional Particle Image Velocimetry (PIV) was then used to measure velocity fields in the resulting vertical (XZ) plane, employing two side-mounted digital CCD cameras to record flow fields within specific regions of interest [i.e. across the sill (Figure 2(a)) and down the sloping face of the obstruction in the estuary/fjordic basin]. This PIV set-up also facilitated the use of Laser Induced Fluorescence (LIF) to consider internal mixing dynamics and entrainment/ detrainment processes across the sill obstruction.

Detailed density profile measurements were measured at key locations across the sill obstruction and within the sea basin using an array of motorized micro-conductivity probes (C1 – C5, Figure 2). A 3D acoustic doppler velocimeter (ADV) probe was also utilized to measure detailed velocity profiles at a similar measurement location to the micro-conductivity probe C2 (i.e. x = -0.5 m), in order to predict gradient Richardson number profiles for the restricted exchange flows generated under different parametric conditions outlined above.

3. RESULTS

3.1 PIV Measurements and Density Profiles

Figure 3 shows typical PIV flow field measurements obtained across the sill obstruction under varying freshwater inflow conditions [i.e. Q_0 = 0, 3, 18 l/s, Figures 3(a) – (c)] for otherwise fixed parametric conditions (i.e. h_s/H = 0.59; $\Delta\rho/\rho$ = 0.0096; Q_1 = 25 l/s). The plots indicate two regions where poor velocity measurements are obtained (i.e. x = -90 to -110 cm and -45 to -65 cm) due to transitions in Plexiglas channel wall panels. However, outside these regions, the strength and thickness of the dense water spillage across the obstruction sill in shown to decrease as the freshwater flow rate Q_1 increases (as indicated by an increase in counter-flowing upper freshwater layer velocities). This suggests that there is significantly increased levels of interfacial mixing and partial blockage of the dense water overflow into the estuary/fjordic basin as Q_0 increases.

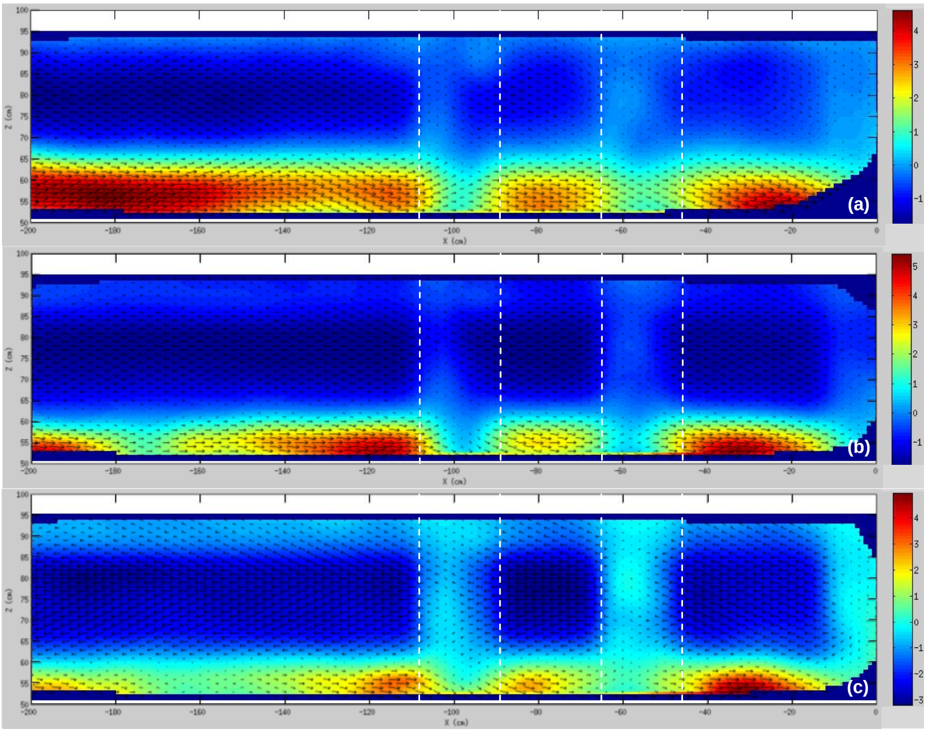

Figure 3. Time-averaged velocity fields across the sill obstruction [PIV window, Figure 2(a)] showing counter-flowing exchange flow generated in estuary run 4 (h_s/H = 0.47, $\Delta\rho/\rho$ = 0.0096) under different Q_0/Q_1 inflow conditions of (a) 0 (i.e. Q_0 = 0); (b) 0.12; (c) 0.72.

Full-depth density profiles $\rho(z)$ were also obtained at two fixed positions in the sea basin (i.e. C1 and C3, x = -3.52 and -3.02 m, respectively, Figure 2) and at three positions across the obstacle sill (i.e. C5, C2 and C4, x = -1.0, -0.5, 0.0 m, Figure 2) for each set of parametric conditions tested during the estuarine runs. Figure 4 shows typical measurements of these profiles, plotted as density excess $(\rho(z) - \rho_0)/(\rho_1 - \rho_0)$, for the exchange flow condition with Q_0 = 0 [Figure 4(a)] and Q_0 = 27 l/s [Figure 4(b)] (for otherwise identical parametric conditions). For the density profiles obtained across the obstruction, there is the clear formation of a sharp interface between the dense water overflow layer across the sill and overlying freshwater layer (for the Q_0 = 0 l/s condition). However, as the freshwater flow rate increase, there is clear evidence of interfacial mixing, particularly close to the estuary/fjordic basin [probe C4, Figure 4(b)]. This again suggests that the counter-flowing freshwater layer is acting to partially block this dense water intrusion.

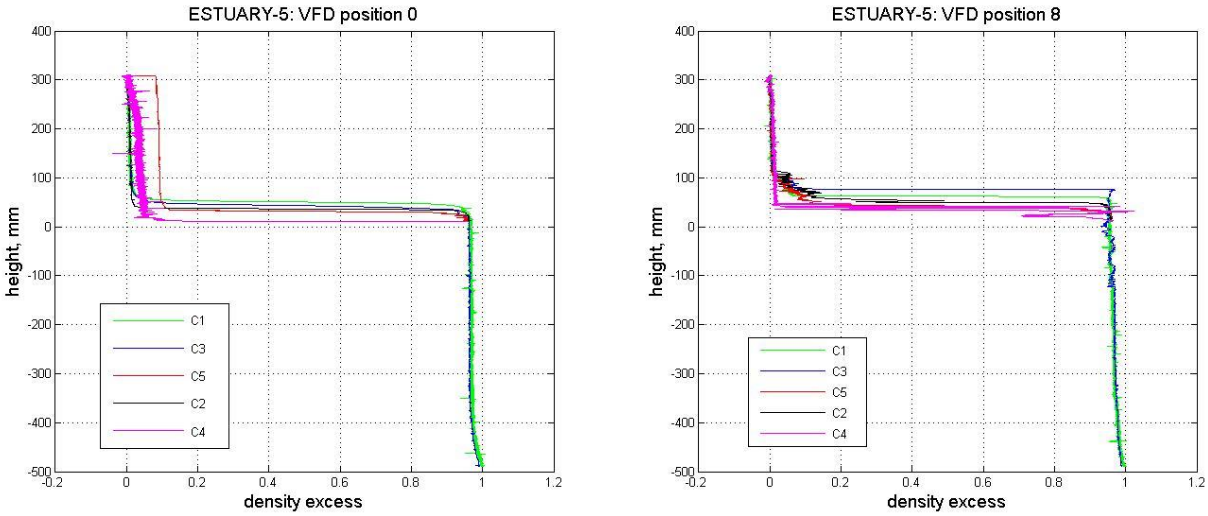

Figure 4. Measured density profiles C1 – C5 [probe positions shown in Figure 2(a) and (b)] generated in estuary run 5 (h_s/H = 0.59, $\Delta\rho/\rho$ = 0.0096) under different Q_0/Q_1 inflow conditions of (a) 0 (i.e. Q_0 = 0) and (b) 0.44. Note that for profiles C2, C4 and C5, the crest elevation (z' = 0) is the lower limit of these profiles.

4. CONCLUSIONS

The parametric experimental study presented herein has investigated the nature of the salt water intrusions across a submerged, rigid, trapezoidal-shaped obstruction, separating a saline water "sea" basin from a semi-enclosed freshwater estuary or stratified fjordic basin, under different freshwater forcing conditions. The primary objectives of this study were to (i) provide new data informing on interfacial mixing and bed boundary processes associated with counter-flowing restricted exchange flows for future validation of advanced numerical models, and (ii) to define parametrically the conditions under which saline water intrusions across the obstruction were arrested. It is also anticipated that the findings from the study will be utilized to develop and apply simple hydraulic models to help interpret the mixing phenomena observed within these large-scale restricted exchange flow experiments.

ACKNOWLEDGMENTS

This work has been supported by European Community's Seventh Framework Programme through the grant to the budget of the Integrating Activity HYDRALAB IV within the Transnational Access Activities, Contract no. 261520.

REFERENCES

Cuthbertson A.J.S., Laanearu J., and Davies P.A. (2006). Buoyancy-driven two-layer exchange flows across a slowly submerging barrier. *Environmental Fluid Mechanics*, 6, 133-151.
Cuthbertson A.J.S., Davies P.A., Coates M.J., and Guo Y. (2004). A modelling study of transient, buoyancy-driven exchange flow over a descending barrier. *Environmental Fluid Mechanics*, 4, 127-155.
Lilover M.J., Lips U., Laanearu J., and Liljebladh B. (1998). Flow regime in the Irbe Strait. *Aquatic Sciences*, 60(3), 253-265.
Laanearu J., Vassiljev A., & Davies P.A. (2011). Hydraulic modelling of stratified bi-directional flow in a river mouth. *Engineering and Computational Mechanics (Proc. ICE)*, 164(4), 207-216.
Laanearu J., Koppel T., Soomere T., and Davies P.A. (2007). Joint influence of river stream, water level and wind waves on the height of sand bar in a river mouth. *Nordic Hydrology*, 38(3), 287 - 302.
Lilover M.J., and Stips A. (2008). The variability of parameters controlling the cyanobacteria bloom biomass in the Baltic *Sea. Journal of Marine Systems*, 74, S108 - S115.
Sargent F.E., and Jirka G.H. (1988). Experiments on Saline Wedge. *J. Hydraulic Engineering*. ASCE. 113(10), 1307-1323.